

A compilation of total cross section data on $e^+e^- \rightarrow \text{hadrons}$ and pQCD tests

O. V. Zenin, V. V. Ezhela, S. B. Lugovsky
COMPAS Group, IHEP, Protvino, Russia

M. R. Whalley
HEPDATA Group, Durham University, Durham, UK

K. Kang^{a,b} and S. K. Kang^a
^aKorea Institute for Advanced Study, ^bBrown University

Abstract

All available data on the total cross sections and R -ratio of $e^+e^- \rightarrow \text{hadrons}$ are compiled from the PPDS (DataGuide), PPDS (ReacData) and HEPDATA (Reaction) databases and transformed to a compilation of data on the $e^+e^- \rightarrow \text{quark } \overline{\text{quark}} \rightarrow \text{hadrons}$ in the continuum region which can be used in tests of the parton model and pQCD calculations. This evaluated data compilation is made available in PPDS system and is accessible through the Web. It is shown that current predictions from the parton model and pQCD are well supported by this world “continuum” data compilation which can then be used in future refinements of the $\alpha_s(Q^2)$ as well as $\alpha_{QED}(Q^2)$ evolution forms.

Motivation

Despite the tremendous efforts of experimentalists and phenomenologists devoted to the investigation of hadron production in e^+e^- collisions there is no real integrated view on the experimental situation even for one of the main observables, the total cross section for the reaction $e^+e^- \rightarrow \text{hadrons}$ and the ratio

$$R = \frac{\sigma(e^+e^- \rightarrow \text{hadrons})}{\sigma(e^+e^- \rightarrow \mu^+\mu^-)_{QED}}$$

Some data are published only as cross sections, σ , and others only as R . The situation is more complicated as QED radiative effects to the data have been corrected for in different ways, and to different degrees, in the various data sets. For example, in constructing R experimentalists have used two forms of theoretical calculations, one with $\alpha_{QED}(0)$, or another taking into account the then currently accepted form of evolution of $\alpha_{QED}(Q^2)$. Furthermore, some data were never published in numerical form and have been read by compilers from graphs. The current experimental situation (March 2001) is summarized in Figures 3 and 4.

This aim of this work is firstly to prepare a comprehensive compilation of σ and R transformed, wherever possible, to a unique, and meaningful, style of implementing the pure QED radiative corrections. The second aim is to construct a procedure to extract “continuum data sets” where the direct comparison of the parton model with different variants of the pQCD corrections will be conclusive. In selecting data for the compilation we use expert assessments from recent reviews and works dealing with precision estimation of running $\alpha_{QED}(Q^2)$ and $\alpha_S(Q^2)$ (see [6], [7], [8], [9], [10], [11], [12], [13], [14]).

1 Data selection and normalizations

1.1 General overview

The data, which have been published in [24]-[112], were extracted in numerical form from the PPDS RD [113] database and from the Reaction database of HEPDATA system [114]. The following criteria were then applied to define suitable data sets:

- All preliminary data are excluded;
- Data obtained under incomplete kinematical conditions, and not extrapolated to the complete kinematic region, are excluded;
- Data in the form of dense energy scans are omitted if the authors published in addition the data averaged over wider energy bins.

The data sets remaining after the above exclusion criteria have been applied, are subdivided into the following six categories:

σ_1^{sd} (Refs. [60] – [67]). Cross section data corrected by their authors for the contributions of two-photon exchange diagrams, the initial state bremsstrahlung and for the initial state vertex loops, but not corrected for the vacuum polarization contribution to the running α_{QED} . These “**semi-dressed**” cross sections correspond to the contribution of the diagram shown on Fig. 1. The full γ/Z propagator, taking

into account all vacuum polarization effects, is denoted on the figure by the bold waved line.

σ_2^{sd} (Refs. [68] – [70]). Cross section data radiatively corrected by their authors according to the procedure of Bonneau and Martin [1]. This procedure included radiative corrections for the initial state radiation, electronic vertex correction, and the correction for the electronic loop in the photon propagator. Thus it partially took into account the vacuum polarization effects also. To obtain from these cross sections the “**semi-dressed**” ones (corresponding to the diagram on Fig. 1) we rescale σ_2^{sd} by a factor $1/(1 - \Delta\alpha_{QED}^e(s))^2$. We suggest that all the cross sections published before 1978 were radiatively corrected according to this procedure.

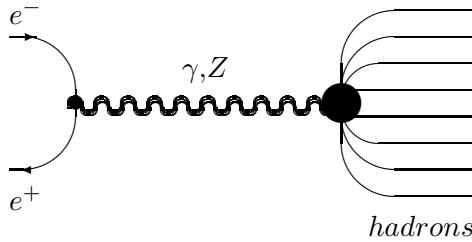


Fig. 1

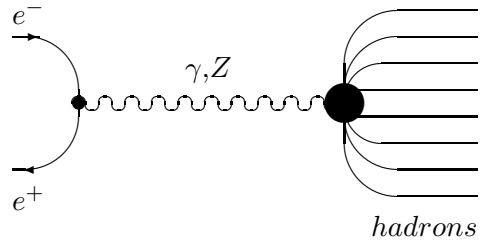


Fig. 2

R_3^{bare} (Ref. [59]). Data on R obtained from measurements of the “**semi-dressed**” (σ_2^{sd}) cross-section divided, by their authors, by the point-like muonic cross section with fixed $\alpha_{QED} = \alpha_{QED}(0)$. We rescale these data by the factor $(\alpha_{QED}(0)/\alpha_{QED}(s))^2/(1 - \Delta\alpha_{QED}^e(s))^2$, to obtain the “**bare**” R -parameter described by the diagram shown on the Fig. 2. The tree-level γ/Z propagator is denoted here by the waved line.

R_4^{bare} (Refs. [24] – [58]). Data on R obtained from measurements of the “**semi-dressed**” (σ_1^{sd}) cross section divided, by their authors, by the point-like muonic cross section, but with the running $\alpha_{QED}(s)$ thus obtaining the “**bare**” R -ratio, which corresponds to the Fig. 2 diagram again.

σ_5^{sd} (Refs. [71] – [81]). LEP I cross section data at the Z peak not corrected for initial state radiation and electronic QED vertex loops, and LEP II – III cross section data at $\sqrt{s} > 130$ GeV with a cut $s'/s = 1 - (\sqrt{s}/2)(1 - 0.7225)$. One can interpret $\sqrt{s'}$ as an effective mass of the propagator after the initial state radiation has reduced the e^+e^- pair center-of-mass energy. Indeed, the definition of s' depends on the assumptions about the initial and final state radiation interference.

These data were rescaled to the “**semi-dressed**” cross section, σ_1^{sd} , defined by the contribution of the Fig. 1 diagram as follows. First, the theoretical cross sections¹ σ_{cut}^{th} and σ_{Born}^{th} were calculated using the ZFITTER 6.30 package² [23] assuming the recommended by PDG [2] values of the standard model parameters. σ_{cut}^{th} means here the cross section measured with cuts applied in the particular experiment and calculated by ZFITTER. σ_{Born}^{th} denotes theoretical cross section, calculated by ZFITTER in the Improved Born Approximation (IBA), that corresponds to the Fig 1 diagram. Then the experimental cross section was multiplied by the factor $\sigma_{Born}^{th}/\sigma_{cut}^{th}$. The results of this rescaling procedure are enlisted in the Tables 3a, 3b.

σ_6^{sd} . Low energy data ($2m_\pi < E_{cm} < 2$ GeV). The treatment of these data is discussed in the following section.

1.2 Low energy data treatment ($2m_\pi < E_{cm} < 2$ GeV)

Our treatment of the cross section, σ_6^{sd} , data in low energy range $2m_\pi < \sqrt{s} < 2$ GeV requires special consideration.

All the cross sections $\sigma(e^+e^- \rightarrow hadrons)$ in this range are obtained via exclusive channel summation and therefore give only a lower estimate of the total hadronic cross section. Below 1 GeV we summed up the 2π and 3π channels from the references [82] – [95] using a linear interpolation of the individual data sets within specific energy regions and combined them to give the total hadron cross sections in these regions. The errors were calculated according to these interpolation and summation procedures.

Such an approach works well if all the data are evenly distributed over \sqrt{s} and have comparable errors. Otherwise if in the given \sqrt{s} interval there are few points of the leading channel with large errors, and this interval is filled more densely by the points of less contributing channels, resonance-like false structures in the total cross section may arise.

The possibility of such false structures is likely for the exclusive channel data in the range $1.4 < \sqrt{s} < 2$ GeV, where we summed the contributions from the channels $\geq 3hadrons$, $\pi^+\pi^-$, K^+K^- , and $K_S K_L$. To avoid these false structures we have determined the sum of exclusive channels not for all points, where at least one channel is measured, but in a fewer number of points, in which the channels yielding the major contributions are measured. In other aspects the summation

¹Values for σ_{cut}^{th} were calculated using ZFITTER subroutine ZUTHSM with argument settings according to the cuts applied in the LEP I-II-III measurements. Values for σ_{born}^{th} were calculated by the same subroutine but with the special flag switching it to calculate the IBA cross sections

²ZFITTER 6.30 Fortran code is available at http://www.ifh.de/~riemann/Zfitter/zfiter6_30.uu .

procedure was the same as the one used for the data below 1 GeV. The exclusive channel data for $1.4 < \sqrt{s} < 2$ GeV are [96] – [112]. The exclusive sum data in the $0.81 < \sqrt{s} < 1.4$ GeV region are taken from [112]. The data used for the exclusive channel summation around ϕ resonance ($0.997 < \sqrt{s} < 1.028$ GeV) were corrected by their authors for the initial state radiation, electronic vertex loops and leptonic 1-loop insertions into the γ propagator. We have properly rescaled these data points to the Fig 1 diagram. In the remaining 0.81–1.4 GeV data their authors applied QED-corrections using the Bonneau and Martin [1] prescription and all these data points were rescaled as in the σ_2^{sd} -case.

2 Data compilations on σ^{sd} and R^{bare}

After the data selection and rescaling, described in Section 1, we assemble the complete data set of the total hadronic cross sections σ^{sd} , normalized to the contribution of the Fig. 1 diagram in accordance with the symbolic relation

$$\sigma^{sd} = \sigma_1^{sd} \cup \sigma_2^{sd} \cup \sigma_5^{sd} \cup \sigma_6^{sd} \cup \left[(R_3^{bare} \cup R_4^{bare}) \cdot \sigma_{QED\ pole, running}^{\mu\mu} \alpha_{QED} \right]$$

and the complete data set for the R -ratios

$$R^{bare} = \frac{\sigma(e^+e^- \rightarrow \text{hadrons})_{Fig.1\ diagram}}{\sigma(e^+e^- \rightarrow \mu^+\mu^-)_{QED\ pole, running\ \alpha_{QED}}}.$$

As described above, in creating compilations which are uniform in the sense of a standardized implementation of pure QED radiative corrections to the “raw” published experimental data, the values of the running $\alpha_{QED}(s)$ and $\Delta\alpha_{QED}^e(s)$ were used. The procedures for obtaining their numerical values and estimates for their uncertainties are described in the Appendix. Both compilations are stored and maintained in the PPDS CS database. Each record in the compilation corresponds to the record of the original data but contains the rescaled data points. Brief descriptions of the applied conversion procedures are stored in the special comment in each record. The σ and R^{bare} compilations obtained by this procedure are shown in the Figs. 5 and 6, respectively.

3 The continuum regions

To be able to pick out the region where the parton model with QCD corrections can be tested we need to consider the relevant theoretical formulae.

3.1 Theoretical relations.

In the parton model, before QCD corrections are applied, the R -ratio is given by

$$R = 3 \sum_q R_q^0 = 3 \sum_q \left[\beta_q \left(1 + \frac{1}{2} (1 - \beta_q^2) \right) \cdot R_q^{VV} + \beta_q^3 R_q^{AA} \right], \quad (1)$$

where

$$\begin{aligned} R_q^{VV} &= e_e^2 e_q^2 + 2e_e e_q \bar{v}_e \bar{v}_q \operatorname{Re} \chi + (\bar{v}_e^2 + \bar{a}_e^2) \bar{v}_q^2 |\chi|^2 \\ R_q^{AA} &= (\bar{v}_e^2 + \bar{a}_e^2) \bar{a}_q^2 |\chi|^2 \end{aligned} \quad (2)$$

with

$$\begin{aligned} \chi &= \frac{1}{16\bar{s}^2\bar{c}^2} \frac{s}{(s - M_Z^2 + iM_Z\Gamma_Z)} \\ \bar{v} &= \sqrt{\rho} (T_3 - 2Q\bar{s}^2) \\ \bar{a} &= \sqrt{\rho} T_3 \\ \rho &= 1 + \frac{3\sqrt{2}G_F}{16\pi^2} m_t^2 + \dots \end{aligned} \quad (3)$$

Here \bar{s}^2, \bar{c}^2 are an effective $\sin^2 \theta_W, \cos^2 \theta_W$ defined through renormalized couplings at $s = M_Z^2$:

$$M_Z^2 = \frac{\pi \cdot \alpha_{QED}(M_Z^2)}{\sqrt{2}G_F \cdot \rho \cdot \bar{s}^2 \cdot \bar{c}^2}. \quad (4)$$

The dominant correction term in ρ originates from t -quark loops in W and Z propagators which result in an $SU(2)$ violation due to the large mass splitting between the b and t quarks [15].

Including QCD loops the expression for R is now (see, e.g. [21], [22]):

$$\begin{aligned} R &= 3 \sum R_q \\ &= 3 \sum \left[R_q^0 + \left(\frac{\alpha_s}{\pi} + \left(\frac{\alpha_s}{\pi} \right)^2 (1.9857 - 0.1153N_f) \right. \right. \\ &\quad \left. \left. - \left(\frac{\alpha_s}{\pi} \right)^3 (6.6368 + 1.2001N_f + 0.0052N_f^2 + 1.2395(\sum Q_q)^2) \right) \times \right. \\ &\quad \left. \times (f_1 R_q^{VV} + f_2 R_q^{AA}) \right] \end{aligned} \quad (5)$$

The coefficients f_1 and f_2 depend only on the quark velocity $\beta = (1 - 4M_q^2/s)^{1/2}$, where M_q is the flavour production threshold mass of the quark q . Schwinger [17] calculated f_1 in the QED context and parameterised it in a form which is accurate enough for our purposes:

$$f_1 = \beta_q \left(1 + \frac{1}{2}(1 - \beta_q^2) \right) \frac{4\pi}{3} \left(\frac{\pi}{2\beta_q} - \frac{3 + \beta_q}{4} \left(\frac{\pi}{2} - \frac{3}{4\pi} \right) \right) \quad (6)$$

Here N_f is a number of active quark flavours. The coefficient f_2 (which have no counterpart in QED) were calculated by Jersak et al [16]. As there is no compact analytical expression for f_2 , we parameterised it as

$$f_2 = a_4\beta_q^4 + a_3\beta_q^3 + (1 - a_4 - a_3)\beta_q^2 \quad (7)$$

with $a_4 = -16$, $a_3 = 17$. From equations (1), (2), (5) one can easily estimate that even assuming a 100% error for f_2 , the relative error of R is less than 10^{-7} at $\sqrt{s} = 10$ GeV and less than 0.5% at the Z pole. As we did not use Z pole data in our fits, it could not be a source of large theoretical errors.

In the massless quark limit, $f_1 = f_2 = 1$. However, at $\sqrt{s} = 35$ GeV for b quarks one has $\beta = 0.963$ whence $f_1 \simeq 1.3$ and $f_2 \simeq 1.7$. Indeed, such a parameterisation of mass effects is valid in QCD only for $\mathcal{O}(\alpha_s)$ order. Now the correct parameterisation is known upto $\mathcal{O}(\alpha_s^3)$ order ([21],[22]), but it was not implemented yet into our programme. It is likely that it results in large enough discrepancies just in the region where α_s/π becomes large.

The following three-loop parameterisation of α_s was chosen here (see, e.g., [18]):

$$\begin{aligned} \ln(Q^2/\Lambda_{MS}^2) = & \frac{4\pi}{\beta_0\alpha_s} - \frac{1}{2} \frac{\beta_1}{\beta_0^2} \ln \left[\left(\frac{4\pi}{\beta_0\alpha_s} \right)^2 + \frac{\beta_1}{\beta_0^2} \left(\frac{4\pi}{\beta_0\alpha_s} \right) + \frac{\beta_2}{\beta_0^3} \right] \\ & - \frac{1}{\Delta} \left(\frac{\beta_1}{\beta_0^2} \right) \tan^{-1} \left[\frac{1}{\Delta} \left(\frac{\beta_1}{\beta_0^2} + \frac{2\beta_2}{\beta_0^3} \left(\frac{\beta_0\alpha_s}{4\pi} \right) \right) \right] \end{aligned} \quad (8)$$

with

$$\begin{aligned} \beta_0 &= 11 - 2N_f/3, \\ \beta_1 &= 2(51 - 19N_f/3), \\ \beta_2 &= (2857 - 5033N_f/9 + 325N_f^2/27)/2, \\ \Delta &= \sqrt{4\beta_2/\beta_0^3 - \beta_1^2/\beta_0^4}. \end{aligned} \quad (9)$$

Here N_f is a number of quark flavours, contributing to the α_s evolution. The onset of a new flavour q takes place at $Q^2 = \mu_q^2 = 4m_q^2$, where, in general, $m_q \neq$

M_q . Here are five different $\Lambda_{\overline{MS}}(N_f)$ corresponding to $N_f = 2, 3, 4, 5, 6$ above the appropriate quark thresholds. To sew up α_s at the thresholds an apparent matching condition for Λ 's was used. Thus at any Q^2 $\alpha_s(Q^2)$ is determined by, say, $\alpha_s(M_Z^2)$, which has been used as a parameter for fits.

We solved this equation at given Q^2 numerically by rewriting it in the form $x = f(x)$, where $x = 4\pi/(\beta_0\alpha_s)$. It enabled us to obtain correct α_s even at $Q^2/\Lambda^2 \sim 1$, where the expansion by powers of leading logarithms (see, e.g., [13]) is no more valid. At $Q^2/\Lambda^2 \gg 1$ both methods yield the same result. (See Fig. 8)

3.2 Preliminary fit results

In order to check the consistency of the description of the data on

$$R = \sigma(e^+e^- \rightarrow \text{hadrons})/\sigma(e^+e^- \rightarrow \mu^+\mu^-)$$

with the theoretical R -ratio expression we have performed several fits using a sub-set of the total compiled data set of R which is applicable to the perturbative domain. This sub-set of the data is defined by the the following steps:

1. The low energy region $2m_\pi < \sqrt{s} < 2$ GeV is completely excluded;
2. All the data above 70 GeV are excluded, as we did not attempt to perform any fits of Z pole parameters M_Z , Γ_Z , \bar{s}_W^2 and M_{top} . This exclusion justified because these data slightly depend on $\alpha_s(M_Z)$ and quark masses and thus their influence to the fits of these parameters would be rather negligible.
3. Data located closer than 20 Breit–Wigner widths to the narrow hadronic 1^{--} resonances $J/\psi(1S)$, $\psi(2S)$, $\psi(3770)$, $\Upsilon(1S)$, $\Upsilon(2S)$, $\Upsilon(3S)$, $\Upsilon(4S)$, $\Upsilon(10860)$ and $\Upsilon(11020)$ are completely excluded;
4. We also completely exclude SLAC-SPEAR-MARK-1 data [41] in the 2.6 GeV $< \sqrt{s} < 7.8$ GeV range. These data systematically lie $\simeq 15\%$ above other experiments in the same interval.

Some remarks on our treatment of the quark masses should be made here. We distinguished the $\gamma^* \rightarrow q\bar{q}$ production threshold masses M_q and the QCD quark masses m_q . The M_q 's should be set actually equal to the masses of the lightest mesons, above which pair production threshold the onset of the new flavour q gives rise to the continuum cross section $\sigma(e^+e^- \rightarrow \text{hadrons})$. The latter are just $m_q = \mu_q/2$, where μ_q is the energy scale at which the onset of the new flavour q in the evolution of α_s takes place. We fitted only M_c and M_b , the other M_q and m_q were fixed at their central PDG values.

The standard χ^2 of the least squares method with weights as inverse squared total experimental errors (neglecting correlations in data) is used with the standard MINUIT[115] package.

After performing the exclusions 1) – 4) we fixed $\alpha_s(M_Z)$, M_Z , Γ_Z , \bar{s}_W^2 , M_q ($q = u, d, s, t$), m_q ($q = u, d, s, c, b, t$) at the values shown in the Table 1, leaving as free parameters just M_c and M_b . Another essential feature of our fit **(I)** was that we retained as a free parameters left and right boundaries of the interval $[\sqrt{s_1}, \sqrt{s_2}]$, $3.0 \leq \sqrt{s_1} \leq 3.670$ GeV, $3.870 \leq \sqrt{s_2} \leq 5.0$ GeV, which was to be excluded from the data set in the process of χ^2/dof minimization itself.³ Thus, the number of degrees of freedom was also variable during this fit. Such a χ^2/dof minimization procedure cancelled possible arbitrariness in the exclusions of broad resonances in the region above $c\bar{c}$ threshold.

In the fit **(II)** we released $\alpha_s(M_Z)$, fixing at the same time the excluded region $\sqrt{s} = 3.09 \div 4.44$ GeV. M_c , M_b were fixed at their fitted values obtained in the fit **(I)**. Fit **(II)** results in too high value $\alpha_s(M_Z) = 0.128 \pm 0.032$.

Preliminary fit parameter settings and results are enlisted in the Table 1. The reduced data set is shown on the Fig. 7. The references used for our fit and the list of excluded \sqrt{s} regions containing hadronic resonances are quoted in the Table 2.

4 Summary. Assessed Data Compilations.

In summary:

- We have created two complementary computerized “raw” data compilations on σ and R with data presented as in the original publications in all cases except the low energy subsample. In the low energy region, where there are no direct measurements of the total cross section, we obtain estimates of the total cross section either as the sum of exclusive channels or as the sum of the two-body exclusive channels with the data on $e^+ e^- \rightarrow \geq 3hadrons$.
- On the basis of above two data sets we have created compilations of data on σ^{sd} (corrected to the level of Fig 1) and R^{bare} (corrected to the level of Fig. 2) with one-to-one correspondence between the data points. Where necessary

³Narrow ψ family resonances between 3 and 4 GeV were excluded by default. Somewhat controversial is the question, whether the gaps between ψ 's can be really treated as the continuum regions. R ratio demonstrates no step up until $\sqrt{s} = 3.9 - 4.0$ GeV, just at the left knee of the broad $\psi(4040)$ resonance, where the continuum approximation of R does not work. Nevertheless, this step results in the fitted c -quark mass $M_c = 1.971$ (see fit **(III)** in the Table 1).

In pQCD fits, performed in Refs. [19], [9] the interval $3.0 < \sqrt{s} < 4.0$ GeV with the resonances excluded was treated as a continuum.

the data have been rescaled to the standard style of implementing the pure QED radiative corrections to the initial state and to photonic propagator to produce a data set which is suitable for tests of the parton model with pQCD corrections for R^{bare} , and to be able to obtain more reliable estimates for $\Delta\alpha_{QED}^{had}(Q^2)$.

- From the total data compilation on R^{bare} we have defined a “continuum” data compilation sub-set which can be used in conjunction with other data in the refinements of the $\alpha_s(Q^2)$ evolution and possibly in the global fits of the Standard Model.

All data files are accessible by:

<http://wwwppds.ihep.su:8001/comphp.html>

and will be accessible from the PDG site soon.

Acknowledgements

We are pleased to thank: R.Yu. Pirogov (for the participation in the early stage of the work); Yu.F. Pirogov for the discussions of the theory aspects; S.R. Slabospitsky, the COMPAS ReacData manager for his kind help; D.E. Groom and R.M. Barnett for the fruitful discussions and encouragements; Z.G. Zhao and Y.S. Zhu for providing us the BES numerical data, and finally to V.S. Lugovsky for providing us the dynamical Web graphic access to CS database. The HEPDATA database project is funded by a grant from the PPARC(UK).

5 Appendix. Running α_{QED} and $\Delta\alpha_{QED}^{had}$

As mentioned above, the authors of the original papers have published data in different forms which required the calculation of several types of factors, containing $\alpha_{QED}(s)$, to rescale the data to, say, “bare” R -ratios. $\alpha_{QED}(s)$ can be expressed in the form (see: [3], [4], [5], [7])

$$\begin{aligned}\alpha_{QED}(s) &= \frac{\alpha(0)}{1 - \Delta\alpha(s)}, \\ \Delta\alpha(s) &= \Delta\alpha^{had}(s) + \Delta\alpha^{lep}(s),\end{aligned}\tag{10}$$

where $\Delta\alpha^{had}(s)$, $\Delta\alpha^{lep}(s)$ are hadronic and leptonic contributions to the QED vacuum polarization, respectively.

$\Delta\alpha^{lep}(s)$ is well determined in perturbative QED as a sum of leptonic loop contributions,

$$\Delta\alpha^{lep}(s) = \sum_{l=e,\mu,\tau} \frac{\alpha(0)}{3\pi} \left[\ln \frac{s}{m_l^2} - \frac{5}{3} + \mathcal{O}\left(\frac{m_l^2}{s}\right) \right]. \quad (11)$$

The situation with $\Delta\alpha^{had}(s)$ is more complicated due to an essentially non-perturbative character of the strong interaction at low energy scales. Using the unitarity condition and the analyticity of the scattering amplitudes, one can express $\Delta\alpha^{had}(s)$ in the form of a subtracted dispersion relation (see, e.g., [5], [7])

$$\Delta\alpha^{had}(s) = -\frac{\alpha(0)s}{3\pi} \int_{4m_\pi^2}^{\infty} \frac{R(s')ds'}{s'(s'-s-i0)}, \quad (12)$$

where $R(s)$ is the “bare” hadronic R -ratio.

This relation allows to effectively combine for its evaluation the $pQCD$ R -ratios in the continuum \sqrt{s} intervals and experimental R data in the non-perturbative ones.

We have evaluated the dispersion integral as

$$\Delta\alpha^{had}(s) = -\frac{\alpha(0)s}{3\pi} \left[\int_{4m_\pi^2}^{\sqrt{s_{cut}}} \frac{R_{bare}^{data}(s')ds'}{s'(s'-s-i0)} + \int_{\sqrt{s_{cut}}}^{\infty} \frac{3\sum_q Q_q^2 ds'}{s'(s'-s-i0)} \right], \quad (13)$$

where the first integral was calculated numerically as a trapezoidal sum over the weighted average of experimental R points in the range $2m_\pi < \sqrt{s'} < \sqrt{s_{cut}} = 19.5$ GeV⁴

Our numerical evaluation procedure is in general similar to the one applied in Ref. [7], except that we performed the trapezoidal integration over all resonances, except $\phi(1020)$.⁵

⁴Choosing S_{cut} we must satisfy at least the following two requirements:

- 1) S_{cut} should lie well above all the hadronic resonances, i.e. 1-loop perturbative QED can be used to calculate hadronic vacuum polarization at $s > s_{cut}$;
- 2) there should be enough densely distributed experimental points at $s < s_{cut}$ for the trapezoidal numerical evaluation of the dispersion integral over $2m_\pi < \sqrt{s} < \sqrt{s_{cut}}$.

As there are few experimental points in the interval $13 < \sqrt{s} < 30$ GeV, $\sqrt{s_{cut}} = 19.5$ GeV appears to be a compromise between these requirements.

⁵As the calculation of R_{bare}^{data} from the original σ and R data (see subsection 1.1) in turn requires the evaluation of $\Delta\alpha^{had}(s)$, we applied the following simple iterative procedure.

We obtain here $\Delta\alpha^{had}(M_Z^2) = 0.0271 \pm 0.0004(\text{exp.})$, being consistent with the latest known to us results 0.027382 ± 0.000197 and 0.027612 ± 0.000220 , obtained with two methodically different low energy data sets in Ref. [20].

The behaviour of $\Delta\alpha^{lep}$, $\Delta\alpha_{(1\text{-loop } QED)}^{had}$ and $\Delta\alpha_{(dispersion)}^{had}$ is depicted in Fig. 9.

Taking as a zero approximation $R(s)$, obtained from the original data using 1-loop perturbative $\alpha_{QED}(s)$, we evaluate $\Delta\alpha^{had(1)}(s)$. Using the latter, we compute the next approximation of $R(s)$ from the original data, the evaluate the integral again to obtain $\Delta\alpha^{had(2)}(s)$, and so on. This process converges well even in resonance regions after 3 iterations. We restricted ourselves to 5 iterations. (For such a number the finite machine precision is likely to result in the error, much less than the error of the method itself).

Table 1. Fit results in the defined “continuum” regions. Adjustable parameters are shown in bold.

Parameter	I	II	III
$\alpha_s(M_Z^2)$	0.1181	0.128(32)	0.126(37)
M_Z	91.187	91.187	91.187
Γ_Z	2.4944	2.4944	2.4944
\bar{s}^2	0.23117	0.23117	0.23117
M_t	174.3	174.3	174.3
M_u	0.140	0.140	0.140
M_d	0.140	0.140	0.140
M_s	0.492	0.492	0.492
M_c	1.500(18)	1.5	1.9710(1)
M_b	5.23 ± 1.16	5.23	6.0 ± 1.4
m_u	0.003	0.003	0.003
m_d	0.006	0.006	0.006
m_s	0.120	0.120	0.120
m_c	1.2	1.2	1.2
m_b	4.2	4.2	4.2
m_t	174.3	174.3	174.3
Excluded	$2m_\pi \div 2.0$ 3.093 ÷ 3.113	$2m_\pi \div 2.0$	$2m_\pi \div 2.0$ 3.093 ÷ 3.113 3.684 ÷ 3.688 3.670 ÷ 3.870
	3.175(247) ÷ 4.319(105)	3.09 ÷ 4.44	4.000 ÷ 4.400
intervals	\sqrt{S}		
	9.450 ÷ 9.470	9.450 ÷ 9.470	9.450 ÷ 9.470
	10.000 ÷ 10.025	10.000 ÷ 10.025	10.000 ÷ 10.025
	10.34 ÷ 10.37	10.34 ÷ 10.37	10.34 ÷ 10.37
	10.52 ÷ 10.64	10.52 ÷ 10.64	10.52 ÷ 10.64
	10.75 ÷ 10.97	10.75 ÷ 10.97	10.75 ÷ 10.97
	11.00 ÷ 11.20	11.00 ÷ 11.20	11.00 ÷ 11.20
70 ÷ 188.7	70 ÷ 188.7	70 ÷ 188.7	
χ^2/dof	0.690	0.665	0.822

Table 2. References of preliminary candidate data to form the continuum domain.

Ref. No.	Data type	N_{points}	E_{min}	E_{max}
[58]	R	85	2.00	4.80
[69]	σ	1	2.23	2.23
[70]	σ	11	2.40	5.00
[57]	R	6	2.60	5.00
[33]	R	2	3.598	3.886
[59]	R	33	3.6025	5.1950
[27]	R	27	3.878	4.496
[30]	R	15	5.00	7.40
[49]	R	31	7.30	10.29
[39]	R	3	7.440	9.415
[42]	σ	13	9.30	9.48
[48]	R	1	9.36	9.36
[46]	R	1	9.39	9.39
[56]	R	1	9.51	9.51
[37]	R	1	10.04	10.04
[38]	R	1	10.43	10.43
[44]	R	1	10.49	10.49
[50]	R	12	12.00	41.40
[36]	R	7	12.00	31.25
[40]	R	14	12.00	36.00
[35]	R	12	12.00	35.80
[43]	R	20	12.00	46.47
[52]	R	18	12.00	46.47
[24]	R	9	14.00	46.60
[31]	R	4	14.03	43.70
[47]	R	1	29.00	29.00
[26]	R	1	29.00	29.00
[34]	R	1	31.57	31.57
[55]	R	1	34.85	34.85
[32]	R	2	34.86	42.72
[51]	R	2	41.45	44.20
[28]	R	12	50.00	61.40
[25]	R	2	50.00	52.00
[29]	R	13	50.00	61.40
[66]	σ	9	57.37	59.84
[67]	σ	1	57.77	57.77
[45]	R	2	63.60	64.00

Table 3a. ZFITTER rescaling results for the Z pole.

\sqrt{s} , GeV	σ_{cut}^{th} [nb]	σ_{born}^{th} [nb]	σ^{exp} [mb]	$\sigma^{exp} \cdot (\sigma_{born}^{th}/\sigma_{cut}^{th})$ [mb]
88.22300	0.44967E+01	0.60846E+01	0.44800E-05	0.60619E-05
88.22300	0.44967E+01	0.60846E+01	0.46100E-05	0.62378E-05
88.22400	0.44992E+01	0.60881E+01	0.46300E-05	0.62651E-05
88.23101	0.45168E+01	0.61131E+01	0.44600E-05	0.60363E-05
88.27800	0.46369E+01	0.62843E+01	0.50400E-05	0.68306E-05
88.46400	0.51600E+01	0.70320E+01	0.51500E-05	0.70183E-05
88.46400	0.51600E+01	0.70320E+01	0.54700E-05	0.74544E-05
88.48001	0.52091E+01	0.71020E+01	0.52200E-05	0.71169E-05
88.48101	0.52121E+01	0.71064E+01	0.53500E-05	0.72944E-05
89.21701	0.83923E+01	0.11703E+02	0.84100E-05	0.11728E-04
89.22200	0.84219E+01	0.11746E+02	0.84800E-05	0.11827E-04
89.22600	0.84458E+01	0.11781E+02	0.84300E-05	0.11759E-04
89.23600	0.85058E+01	0.11868E+02	0.85200E-05	0.11888E-04
89.28300	0.87956E+01	0.12290E+02	0.96800E-05	0.13526E-04
89.45500	0.99723E+01	0.14007E+02	0.99900E-05	0.14032E-04
89.45500	0.99723E+01	0.14007E+02	0.10010E-04	0.14060E-04
89.47000	0.10084E+02	0.14170E+02	0.10150E-04	0.14262E-04
89.47200	0.10099E+02	0.14192E+02	0.10130E-04	0.14235E-04
90.20800	0.17921E+02	0.25591E+02	0.17860E-04	0.25505E-04
90.21200	0.17977E+02	0.25672E+02	0.18230E-04	0.26034E-04
90.21701	0.18047E+02	0.25773E+02	0.18000E-04	0.25706E-04
90.21701	0.18047E+02	0.25773E+02	0.18590E-04	0.26549E-04
90.22600	0.18173E+02	0.25956E+02	0.18740E-04	0.26765E-04
90.22700	0.18188E+02	0.25976E+02	0.18320E-04	0.26165E-04
90.22800	0.18202E+02	0.25996E+02	0.18210E-04	0.26008E-04
90.23800	0.18343E+02	0.26201E+02	0.18680E-04	0.26681E-04
90.24000	0.18372E+02	0.26242E+02	0.18830E-04	0.26896E-04
90.28400	0.19005E+02	0.27152E+02	0.19560E-04	0.27945E-04
91.03400	0.29394E+02	0.40836E+02	0.29940E-04	0.41594E-04
91.20700	0.30374E+02	0.41415E+02	0.30590E-04	0.41710E-04
91.20800	0.30377E+02	0.41414E+02	0.30100E-04	0.41037E-04
91.21500	0.30396E+02	0.41404E+02	0.30460E-04	0.41491E-04
91.21701	0.30401E+02	0.41400E+02	0.30540E-04	0.41590E-04
91.22200	0.30413E+02	0.41391E+02	0.30330E-04	0.41278E-04
91.22300	0.30415E+02	0.41389E+02	0.30190E-04	0.41082E-04
91.22300	0.30415E+02	0.41389E+02	0.30480E-04	0.41477E-04
91.23001	0.30431E+02	0.41373E+02	0.30440E-04	0.41386E-04
91.23800	0.30447E+02	0.41352E+02	0.30630E-04	0.41601E-04
91.23900	0.30448E+02	0.41349E+02	0.29960E-04	0.40686E-04

Table 3a (continued). ZFITTER rescaling results for the Z pole.

\sqrt{s} , GeV	σ_{cut}^{th} [nb]	σ_{born}^{th} [nb]	σ^{exp} [mb]	$\sigma^{exp} \cdot (\sigma_{born}^{th}/\sigma_{cut}^{th})$ [mb]
91.25400	0.30472E+02	0.41300E+02	0.30450E-04	0.41270E-04
91.25400	0.30472E+02	0.41300E+02	0.30460E-04	0.41284E-04
91.28000	0.30494E+02	0.41187E+02	0.30440E-04	0.41113E-04
91.28900	0.30497E+02	0.41139E+02	0.30860E-04	0.41629E-04
91.29400	0.30497E+02	0.41111E+02	0.30450E-04	0.41048E-04
91.52900	0.29641E+02	0.38504E+02	0.29210E-04	0.37945E-04
91.95201	0.25217E+02	0.30140E+02	0.25310E-04	0.30251E-04
91.95301	0.25205E+02	0.30119E+02	0.24780E-04	0.29611E-04
91.96701	0.25030E+02	0.29821E+02	0.24640E-04	0.29356E-04
91.96900	0.25005E+02	0.29779E+02	0.24690E-04	0.29403E-04
92.20700	0.22038E+02	0.24922E+02	0.21830E-04	0.24686E-04
92.20900	0.22014E+02	0.24883E+02	0.21570E-04	0.24382E-04
92.21500	0.21941E+02	0.24768E+02	0.21220E-04	0.23954E-04
92.22600	0.21807E+02	0.24558E+02	0.22010E-04	0.24786E-04
92.28200	0.21135E+02	0.23509E+02	0.21240E-04	0.23626E-04
92.56200	0.18034E+02	0.18865E+02	0.16660E-04	0.17428E-04
92.95201	0.14545E+02	0.14006E+02	0.14590E-04	0.14049E-04
92.95301	0.14537E+02	0.13995E+02	0.14120E-04	0.13594E-04
92.96601	0.14437E+02	0.13862E+02	0.14440E-04	0.13865E-04
92.96800	0.14421E+02	0.13841E+02	0.14110E-04	0.13542E-04
93.20800	0.12739E+02	0.11648E+02	0.12580E-04	0.11503E-04
93.20900	0.12733E+02	0.11640E+02	0.12480E-04	0.11409E-04
93.22000	0.12663E+02	0.11551E+02	0.12330E-04	0.11248E-04
93.22800	0.12612E+02	0.11487E+02	0.12380E-04	0.11276E-04
93.28601	0.12254E+02	0.11035E+02	0.11770E-04	0.10599E-04
93.70100	0.10097E+02	0.84120E+01	0.10200E-04	0.84981E-05
93.70201	0.10092E+02	0.84067E+01	0.10070E-04	0.83883E-05
93.71601	0.10030E+02	0.83341E+01	0.10100E-04	0.83921E-05
93.71701	0.10026E+02	0.83289E+01	0.99500E-05	0.82660E-05
94.20201	0.82093E+01	0.62771E+01	0.78200E-05	0.59795E-05
94.20201	0.82093E+01	0.62771E+01	0.79900E-05	0.61094E-05
94.21900	0.81557E+01	0.62189E+01	0.78800E-05	0.60087E-05
94.22300	0.81432E+01	0.62053E+01	0.80600E-05	0.61420E-05
94.27700	0.79772E+01	0.60261E+01	0.75900E-05	0.57336E-05
95.03601	0.61405E+01	0.41416E+01	0.64400E-05	0.43436E-05

Table 3b. ZFITTER rescaling results for the LEP II–III data.

\sqrt{s} , GeV	$\sigma_{cut}^{th} [nb]$	$\sigma_{born}^{th} [nb]$	$\sigma^{exp} [mb]$	$\sigma^{exp} \cdot (\sigma_{born}^{th} / \sigma_{cut}^{th}) [mb]$
130.00000	0.82691E-01	0.82628E-01	0.84200E-07	0.84136E-07
130.11999	0.82294E-01	0.82264E-01	0.79700E-07	0.79670E-07
130.19999	0.82031E-01	0.82022E-01	0.82100E-07	0.82091E-07
130.19999	0.82031E-01	0.82022E-01	0.71600E-07	0.71592E-07
136.08000	0.66194E-01	0.67219E-01	0.66700E-07	0.67732E-07
136.10000	0.66150E-01	0.67177E-01	0.66600E-07	0.67634E-07
136.19999	0.65930E-01	0.66967E-01	0.65100E-07	0.66124E-07
136.19999	0.65930E-01	0.66967E-01	0.58800E-07	0.59725E-07
161.30000	0.34218E-01	0.35777E-01	0.37300E-07	0.38999E-07
161.30000	0.34218E-01	0.35777E-01	0.40900E-07	0.42763E-07
161.30000	0.34218E-01	0.35777E-01	0.29940E-07	0.31304E-07
172.10000	0.28336E-01	0.29787E-01	0.30300E-07	0.31852E-07
172.10000	0.28336E-01	0.29787E-01	0.26400E-07	0.27752E-07
172.30000	0.28244E-01	0.29693E-01	0.28200E-07	0.29646E-07
182.69000	0.24017E-01	0.25342E-01	0.23700E-07	0.25007E-07
182.69999	0.24014E-01	0.25338E-01	0.21710E-07	0.22907E-07
182.69999	0.24014E-01	0.25338E-01	0.24700E-07	0.26062E-07
188.63000	0.22095E-01	0.23352E-01	0.22100E-07	0.23358E-07
188.69999	0.22073E-01	0.23330E-01	0.23100E-07	0.24415E-07

References

- [1] G. Bonneau and F. Martin, Nucl. Phys. B **27** (1971) 381.
- [2] D. E. Groom *et al.*, [Particle Data Group Collaboration], Eur. Phys. J. C **15** (2000) 1.
- [3] N. Cabibbo, R. Gatto, Phys. Rev. Lett. **4** (1960) 313;
- [4] N. Cabibbo and R. Gatto, Phys. Rev. **124** (1961) 1577.
- [5] R. B. Nevzorov, A. V. Novikov and M. I. Vysotsky, JETP Lett. **60** (1994) 399 [hep-ph/9405390].
- [6] H. Schopper, D. R. Morrison, V. V. Ezhela, Y. G. Stroganov, O. P. Yushchenko, V. Flaminio and M. R. Whalley, *Berlin, Germany: Springer (1992) 332 p. (Landolt-Boernstein. New Series, 1.14)*.
- [7] S. Eidelman and F. Jegerlehner, Z. Phys. C **67** (1995) 585 [hep-ph/9502298].
- [8] H. Burkhardt and B. Pietrzyk, Phys. Lett. B **356** (1995) 398.
- [9] M. L. Swartz, Phys. Rev. D **53** (1996) 5268 [hep-ph/9509248].
- [10] R. Alemany, M. Davier and A. Hocker, Eur. Phys. J. C **2** (1998) 123 [hep-ph/9703220].
M. Davier, LAL **98-87** (1998), Invited talk given at the “5th Int. Workshop on τ Physics,” Santander (Spain), Sep. 14-17, 1998.
- [11] M. Davier and A. Hocker, Phys. Lett. B **435** (1998) 427 [hep-ph/9805470].
- [12] S. Bethke, J. Phys. G **26** (2000) R27 [hep-ex/0004021].
- [13] I. Hinchliffe and A. V. Manohar, Ann. Rev. Nucl. Part. Sci. **50** (2000) 643 [hep-ph/0004186].
- [14] Z.G. Zhao, Int. J. Mod. Phys. A **15** (2000) 3739.
- [15] M. Veltman, Nucl. Phys. B **123** (1977) 89.
- [16] J. Jersak, E. Laermann and P. M. Zerwas, Phys. Lett. B **98** (1981) 363.
- [17] J. Schwinger, “Particles, Sources And Fields.” Addison-Wesley, 1970. 3v.
- [18] R. Marshall, Z. Phys. C **43** (1989) 595.
- [19] A. D. Martin and D. Zeppenfeld, Phys. Lett. B **345** (1995) 558 [hep-ph/9411377].

- [20] A. D. Martin, J. Outhwaite and M. G. Ryskin, Phys. Lett. B **492** (2000) 69 [hep-ph/0008078].
 - [21] K. G. Chetyrkin, J. H. Kuhn and A. Kwiatkowski, Phys. Rept. **277** (1996) 189.
 - [22] K. G. Chetyrkin, R. V. Harlander and J. H. Kuhn, Nucl. Phys. B **586** (2000) 56 [hep-ph/0005139].
 - [23] D. Bardin, P. Christova, M. Jack, L. Kalinovskaya, A. Olchevski, S. Riemann and T. Riemann, Comput. Phys. Commun. **133** (2001) 229 [hep-ph/9908433].
- R-ratio data with proper radiative corrections. R_4^{bare} .**
- [24] H. J. Behrend *et al.*, [CELLO Collaboration], Phys. Lett. B **183** (1987) 400.
 - [25] H. Yoshida *et al.*, [Venus Collaboration], Phys. Lett. B **198** (1987) 570.
 - [26] E. Fernandez *et al.*, [SLAC-PEP-006, MAC collaboration], Phys. Rev. D **31** (1985) 1537.
 - [27] A. Osterheld *et al.*, [SLAC-SP-030, CRYSTAL BALL Collaboration], SLAC-PUB-4160.
 - [28] I. Adachi *et al.*, [TOPAZ Collaboration], Phys. Lett. B **234** (1990) 525.
 - [29] T. Kumita *et al.*, [AMY Collaboration], Phys. Rev. D **42** (1990) 1339.
 - [30] C. Edwards *et al.*, [SLAC-SP-030, Crystall Ball Collaboration], SLAC-PUB-5160.
 - [31] W. Braunschweig *et al.*, [TASSO Collaboration], Z. Phys. C **47** (1990) 187.
 - [32] H. J. Behrend *et al.*, [CELLO Collaboration], Phys. Lett. B **144** (1984) 297.
 - [33] P. A. Rapidis *et al.*, [SLAC-SP-026, SMAG-LGW Collaboration], Phys. Rev. Lett. **39** (1977) 526.
 - [34] D. P. Barber *et al.*, [DESY-PETRA, MARK-J Collaboration], Phys. Lett. B **85** (1979) 463.
 - [35] D. P. Barber *et al.*, [DESY-PETRA, MARK-J Collaboration], Phys. Rept. **63** (1980) 337.

- [36] R. Brandelik *et al.*, [TASSO Collaboration], Z. Phys. C **4** (1980) 87.
- [37] P. Bock *et al.*, [DESY-Hamburg-Heidelberg-Munich Collaboration], Z. Phys. C **6** (1980) 125.
- [38] E. Rice *et al.*, [CESR-CUSB Collaboration], Phys. Rev. Lett. **48** (1982) 906.
- [39] B. Niczyporuk *et al.*, [DESY-DORIS, LENA Collaboration], Z. Phys. C **15** (1982) 299.
- [40] R. Brandelik *et al.*, [TASSO Collaboration], Phys. Lett. B **113** (1982) 499.
- [41] J. Siegrist *et al.*, Phys. Rev. D **26** (1982) 969.
- [42] L. Criegee and G. Knies, [PLUTO Collaboration], Phys. Rept. **83** (1982) 151.
- [43] B. Naroska, [DESY-PETRA, JADE Collaboration], Phys. Rept. **148** (1987) 67.
- [44] R. Giles *et al.*, [CESR-CLEO Collaboration], Phys. Rev. D **29** (1984) 1285.
- [45] K. Abe *et al.*, [VENUS Collaboration], Phys. Lett. B **246** (1990) 297.
- [46] Z. Jakubowski *et al.*, [DESY-DORIS, Crystal Ball Collaboration], Z. Phys. C **40** (1988) 49.
- [47] C. Von Zanthier *et al.*, [SLAC-PEP-005, MARK-II Collaboration], Phys. Rev. D **43** (1991) 34.
- [48] H. Albrecht *et al.*, [ARGUS Collaboration], Z. Phys. C **54** (1992) 13.
- [49] A. E. Blinov *et al.*, [NOVOSIBIRSK-VEPP-4, MD-1 Experiment], Z. Phys. C **70** (1996) 31.
- [50] M. Althoff *et al.*, [TASSO Collaboration], Z. Phys. C **22** (1984) 307.
- [51] M. Althoff *et al.*, [TASSO Collaboration], Phys. Lett. B **138** (1984) 441.
- [52] B. Adeva *et al.*, [DESY-PETRA, Mark-J Collaboration], Phys. Rev. D **34** (1986) 681.
- [53] R. H. Schindler, [SLAC-SP-029, MARK II Collaboration], SLAC-R-0219.
- [54] R. Ammar *et al.*, [CLEO Collaboration], Phys. Rev. D **57** (1998) 1350 [hep-ex/9707018].

- [55] D. P. Barber *et al.*, [DESY-PETRA, MARK-J Collaboration], Phys. Lett. B **108** (1982) 63.
 - [56] H. Albrecht *et al.*, [DESY-DORIS, DASP Collaboration], Phys. Lett. B **116** (1982) 383.
 - [57] J. Z. Bai *et al.*, [BES Collaboration], Phys. Rev. Lett. **84** (2000) 594 [hep-ex/9908046].
 - [58] J. Z. Bai *et al.*, [BES Collaboration], hep-ex/0102003.
R-ratio data, radiatively corrected according to Bonneau/Martin. R_3^{bare} .
 - [59] R. Brandelik *et al.*, [DASP Collaboration], Phys. Lett. B **76** (1978) 361.
 σ data with proper radiative corrections. σ_1^{sd} .
 - [60] C. Berger *et al.*, [PLUTO Collaboration], Z. Phys. C **1** (1979) 343.
 - [61] D. Andrews *et al.*, [CESR-CLEO Collaboration], Phys. Rev. Lett. **50** (1983) 807.
 - [62] R. Giles *et al.*, [CESR-CLEO Collaboration], Phys. Rev. Lett. **50** (1983) 877.
 - [63] J. K. Bienlein *et al.*, Phys. Lett. B **78** (1978) 360.
 - [64] A. Boyarski *et al.*, Phys. Rev. Lett. **34** (1975) 1357.
 - [65] J. Z. Bai *et al.*, [BES Collaboration], Phys. Lett. B **355** (1995) 374.
 - [66] K. Abe *et al.*, [TOPAZ Collaboration], Phys. Lett. B **304** (1993) 373.
 - [67] K. Miyabayashi *et al.*, [TOPAZ Collaboration], Phys. Lett. B **347** (1995) 171.
 σ data, radiatively corrected according to Bonneau/Martin. σ_2^{sd} .
 - [68] G. Cosme *et al.*, [ORSAY-ACO Collaboration], Phys. Lett. B **48** (1974) 155.
 - [69] B. Bartoli *et al.*, [FRAS-ADONE, MEA Collaboration], Phys. Lett. B **58** (1975) 478.
 - [70] J. E. Augustin *et al.*, [SLAC-SP-017, SMAG Collaboration], Phys. Rev. Lett. **34** (1975) 764.
- σ data, from LEPI, LEPII-III. σ_5^{sd} .**

- [71] P. D. Acton *et al.*, [OPAL Collaboration], Z. Phys. C **58** (1993) 219.
 - [72] D. Buskulic *et al.*, [ALEPH Collaboration], Z. Phys. C **60** (1993) 71.
 - [73] P. Abreu *et al.*, [DELPHI Collaboration], Nucl. Phys. B **417** (1994) 3.
 - [74] P. Abreu *et al.*, [DELPHI Collaboration], Nucl. Phys. B **418** (1994) 403.
 - [75] M. Acciarri *et al.*, [L3 Collaboration], Z. Phys. C **62** (1994) 551.
 - [76] G. Alexander *et al.*, [OPAL Collaboration], Z. Phys. C **52** (1991) 175.
 - [77] G. Abbiendi *et al.*, [OPAL Collaboration], Eur. Phys. J. C **6** (1999) 1 [hep-ex/9808023].
 - [78] P. Abreu *et al.*, [DELPHI Collaboration], Eur. Phys. J. C **11** (1999) 383.
 - [79] R. Barate *et al.*, [ALEPH Collaboration], Eur. Phys. J. C **12** (2000) 183 [hep-ex/9904011].
 - [80] G. Abbiendi *et al.*, [OPAL Collaboration], Eur. Phys. J. C **13** (2000) 553 [hep-ex/9908008].
 - [81] M. Acciarri *et al.*, [L3 Collaboration], Phys. Lett. B **479** (2000) 101 [hep-ex/0002034].
- σ data below 1 GeV. σ_6^{sd} .**
- [82] I. A. Koop *et al.*, [OLYA Collaboration], Budker INP-79-67 (1979)
 - [83] A. Cordier *et al.*, [ORSAY-ACO, DM1 Collaboration], Nucl. Phys. B **172** (1980) 13.
 - [84] I. B. Vasserman *et al.*, [VEPP-2, spark chamber system] Yad. Fiz. **33** (1981) 709.
 - [85] G. V. Anikin *et al.*, [VEPP-2M, CMD Collaboration], IYF-83-85 *Contributed to Int. Symp. on Lepton and Photon Interactions at High Energies, Ithaca, N.Y., Aug 4-9, 1983*.
 - [86] L. M. Kurdadze *et al.*, [VEPP-2M, OLYA Collaboration], Sov. J. Nucl. Phys. **40** (1984) 286.
 - [87] V. L. Auslender *et al.*, [VEPP-2, Spark chamber system], Yad. Fiz. **9** (1969) 114.
 - [88] M. Bernardini *et al.*, [FRASCATI-ADONE, BCF Collaboration], Phys. Lett. B **53** (1974) 384.
 - [89] J. E. Augustin *et al.*, [ORSAY-ACO], Phys. Lett. B **28** (1969) 513.

- [90] D. Benaksas *et al.*, [ORSA-ACO], Phys. Lett. B **42** (1972) 507.
- [91] P. M. Ivanov *et al.*, [VEPP-2M, OLYA Collaboration], Phys. Lett. B **107** (1981) 297.
- [92] D. Benaksas *et al.*, [ORSA-ACO], Phys. Lett. B **39** (1972) 289.
- [93] M. N. Achasov *et al.*, [VEPP-2M, SND Collaboration], hep-ex/9809013.
- [94] M. N. Achasov *et al.*, [VEPP-2M, SND Collaboration], Phys. Lett. B **462** (1999) 365 [hep-ex/9910001].
- [95] R. R. Akhmetshin *et al.*, [VEPP-2M, CMD-2 Collaboration], hep-ex/9904027.

**References used for exclusive channels summation
at energies $1.4 < E_{cm} < 2$ GeV. σ_6^{sd} .**

- [96] J. E. Augustin *et al.*, [DM2 Collaboration], LAL-83-21 *Contributed to Int. Europhysics Conf. on High Energy Physics, Brighton, England, Jul 20-27, 1983*.
- [97] D. Bisello *et al.*, [DM2 Collaboration], Z. Phys. C **39** (1988) 13.
- [98] D. Bisello *et al.*, [DM2 Collaboration], Phys. Lett. B **220** (1989) 321.
- [99] F. Mane, D. Bisello, J. C. Bizot, J. Buon, A. Cordier and B. Delcourt, [ORSA-DCI, DM1 Collaboration], Phys. Lett. B **99** (1981) 261.
- [100] I. A. Koop *et al.*, [OLYA Collaboration], Budker INP-79-67 (1979)
- [101] L. M. Kurdadze *et al.*, [OLYA Collaboration], Sov. J. Nucl. Phys. **40** (1984) 286.
- [102] M. Bernardini *et al.*, [ADONE, BCF Collaboration], Phys. Lett. B **46** (1973) 261.
- [103] M. Grilli *et al.*, [ADONE, MU-PI Collaboration], Nuovo Cim. **13A** (1973) 593.
- [104] C. Bacci *et al.*, [ADONE, 2GAMMA Collaboration], Phys. Lett. B **44** (1973) 533.
- [105] C. Bacci *et al.*, [ADONE, 2GAMMA Collaboration], Phys. Lett. B **58** (1975) 481.
- [106] C. Bacci *et al.*, [ADONE, 2GAMMA Collaboration], Phys. Lett. B **86** (1979) 234.

- [107] B. Esposito *et al.*, [ADONE, MEA Collaboration], “Hadronic Cross-Section In E+ E- Annihilation From 1.45-Gev To 1.80-Gev,” *Lett. Nuovo Cim.* **30** (1981) 65.
- [108] B. Esposito *et al.*, [ADONE, MEA Collaboration], “Multi - Hadron Production In E+ E- Annihilation At 1.45-Gev - 1.61-Gev Cm Energy,” *Lett. Nuovo Cim.* **25** (1979) 5.
- [109] B. Bartoli *et al.*, [ADONE, BOSON Collaboration], *Phys. Rev. D* **6** (1972) 2374
- [110] C. Bacci *et al.*, [ADONE, 2GAMMA Collaboration], *Phys. Lett. B* **38** (1972) 551
- [111] F. Ceradini *et al.*, [ADONE, MU-PI Collaboration], *Phys. Lett. B* **42** (1972) 501
- [112] S. I. Dolinsky *et al.*, [VEPP-2M, ND Collaboration], *Phys. Rept.* **202** (1991) 99.
- [113] <http://wwwppds.ihep.su:8001/ppds.html>
- [114] <http://durpdg.dur.ac.uk/hepdata/>
- [115] F. James and M. Roos, *Comput. Phys. Commun.* **10** (1975) 343.

Received 16 May, 2001

Figure Captions

Fig. 3: World data on the total cross section of $e^+e^- \rightarrow hadrons$ as presented in the original publications.

Fig. 4: World data on the experiment-to-theory ratio $R = \sigma(e^+e^- \rightarrow hadrons)_{experimental} / \sigma(e^+e^- \rightarrow \mu^+\mu^-)_{QED \ simple \ pole}$ as presented in the original publications.

Fig. 5: World data on the total cross section of $e^+e^- \rightarrow hadrons$. Curves are an educative guide. Solid curve is the cross section prediction obtained in the three-loop QCD approximation with the effect of non-zero quark masses taken into account.

Fig. 6: R -ratio. Data set is the same as on the Fig. 5. Solid curve is the R -ratio prediction obtained in the three-loop QCD approximation with the effect of non-zero quark masses taken into account. Dashed curve is a “naive” quark parton model prediction for the R -ratio

Fig. 7: Data set used for the fits.

Fig. 8: A comparison of R -ratio obtained with $\alpha_s(s)$, evaluated by our numerical method (solid curve) and by the method described in [13] (dashed curve).

Fig. 9: The behaviour of $\Delta\alpha_{QED}$. $\Delta\alpha_{had}^{(QED)}$ is the quark contribution to $\Delta\alpha_{(QED)}$ calculated in 1-loop QED. $\Delta\alpha_{had}^{(disp)}$ is a hadronic contribution to $\Delta\alpha_{(QED)}$ calculated using the dispersion integral over $\sigma_{had}(s)$, $2m_\pi < \sqrt{s} < 20$ GeV, and 1-loop QED above 20 GeV.

Figure captions

Fig. 3: World data on the total cross section of $e^+e^- \rightarrow hadrons$ as presented in the original publications.

Fig. 4: World data on the experiment-to-theory ratio $R = \sigma(e^+e^- \rightarrow hadrons)_{experimental} / \sigma(e^+e^- \rightarrow \mu^+\mu^-)_{QED \text{ simple pole}}$ as presented in the original publications.

Fig. 5: World data on the total cross section of $e^+e^- \rightarrow hadrons$. Curves are an educative guide. Solid curve is the cross section prediction obtained in the three-loop QCD approximation with the effect of non-zero quark masses taken into account.

Fig. 6: R -ratio. Data set is the same as on the Fig. 5. Solid curve is the R -ratio prediction obtained in the three-loop QCD approximation with the effect of non-zero quark masses taken into account. Dashed curve is a “naive” quark parton model prediction for the R -ratio

Fig. 7: Data set used for the fits.

Fig. 8: A comparison of R -ratio obtained with $\alpha_s(s)$, evaluated by our numerical method (solid curve) and by the method described in [13] (dashed curve).

Fig. 9: The behaviour of $\Delta\alpha_{QED}$. $\Delta\alpha_{had}^{(QED)}$ is the quark contribution to $\Delta\alpha_{(QED)}$ calculated in 1-loop QED. $\Delta\alpha_{had}^{(disp)}$ is a hadronic contribution to $\Delta\alpha_{(QED)}$ calculated using the dispersion integral over $\sigma_{had}(s)$, $2m_\pi < \sqrt{s} < 20$ GeV, and 1-loop QED above 20 GeV.

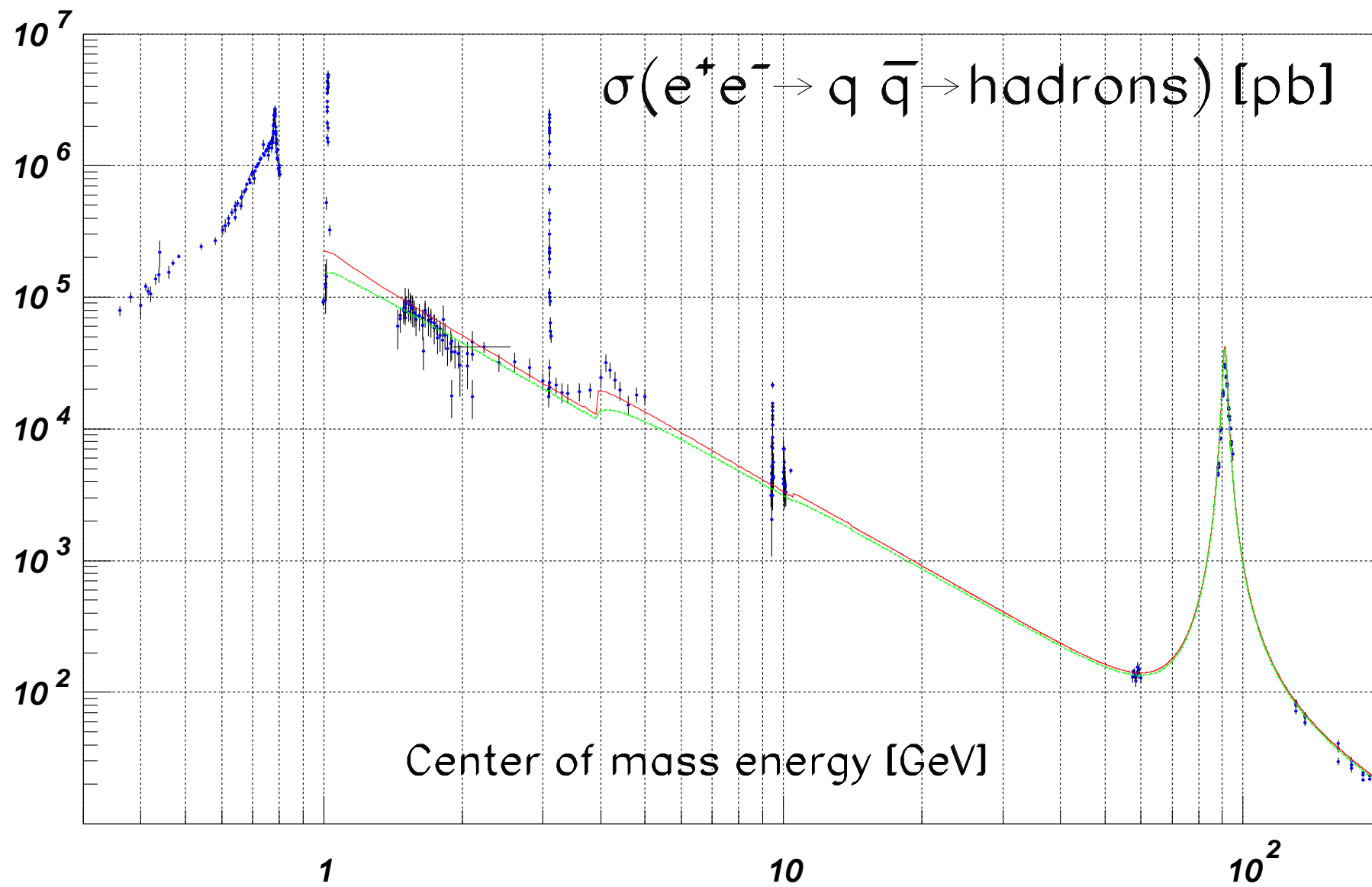


Fig. 3

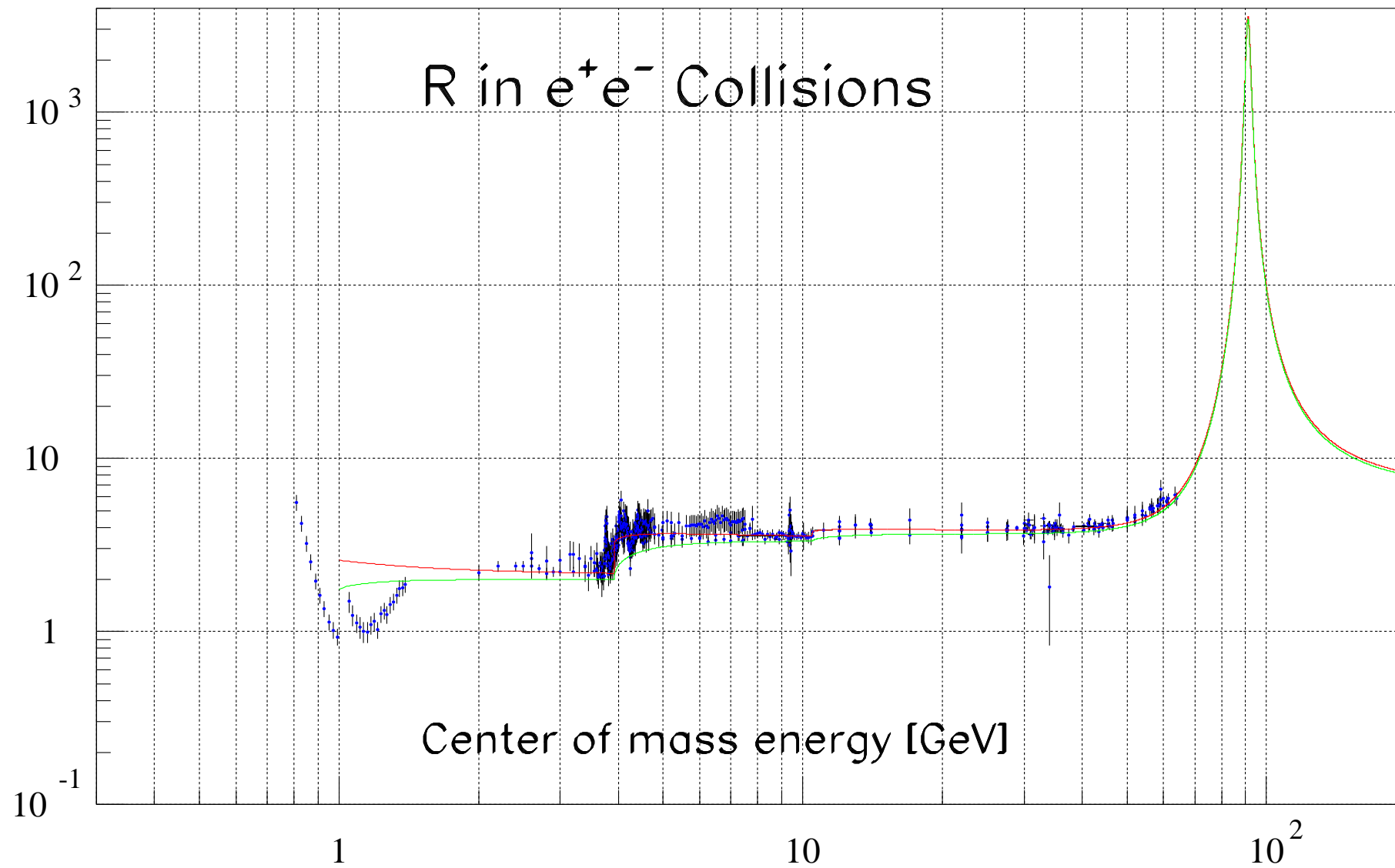


Fig. 4

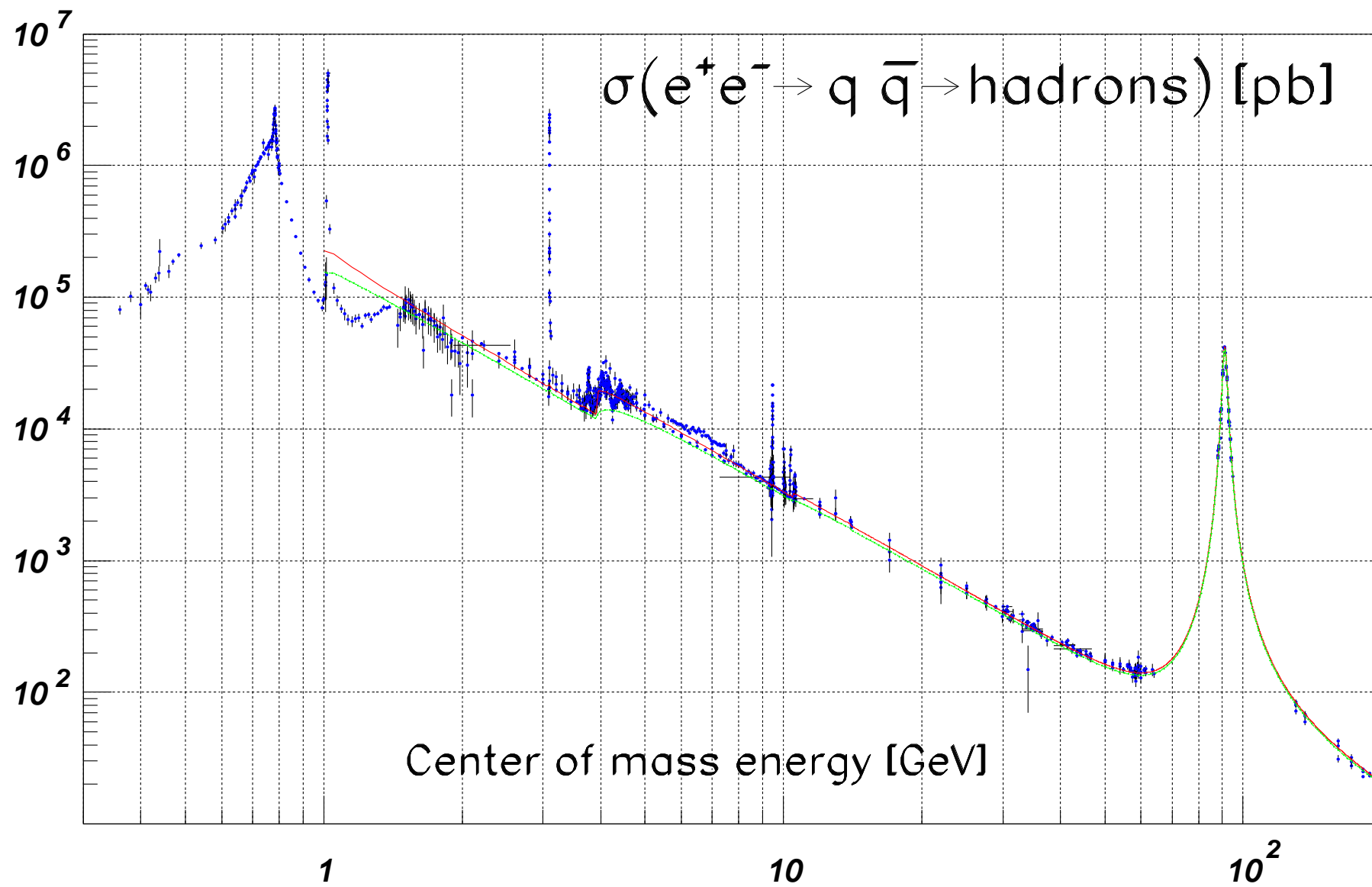


Fig. 5

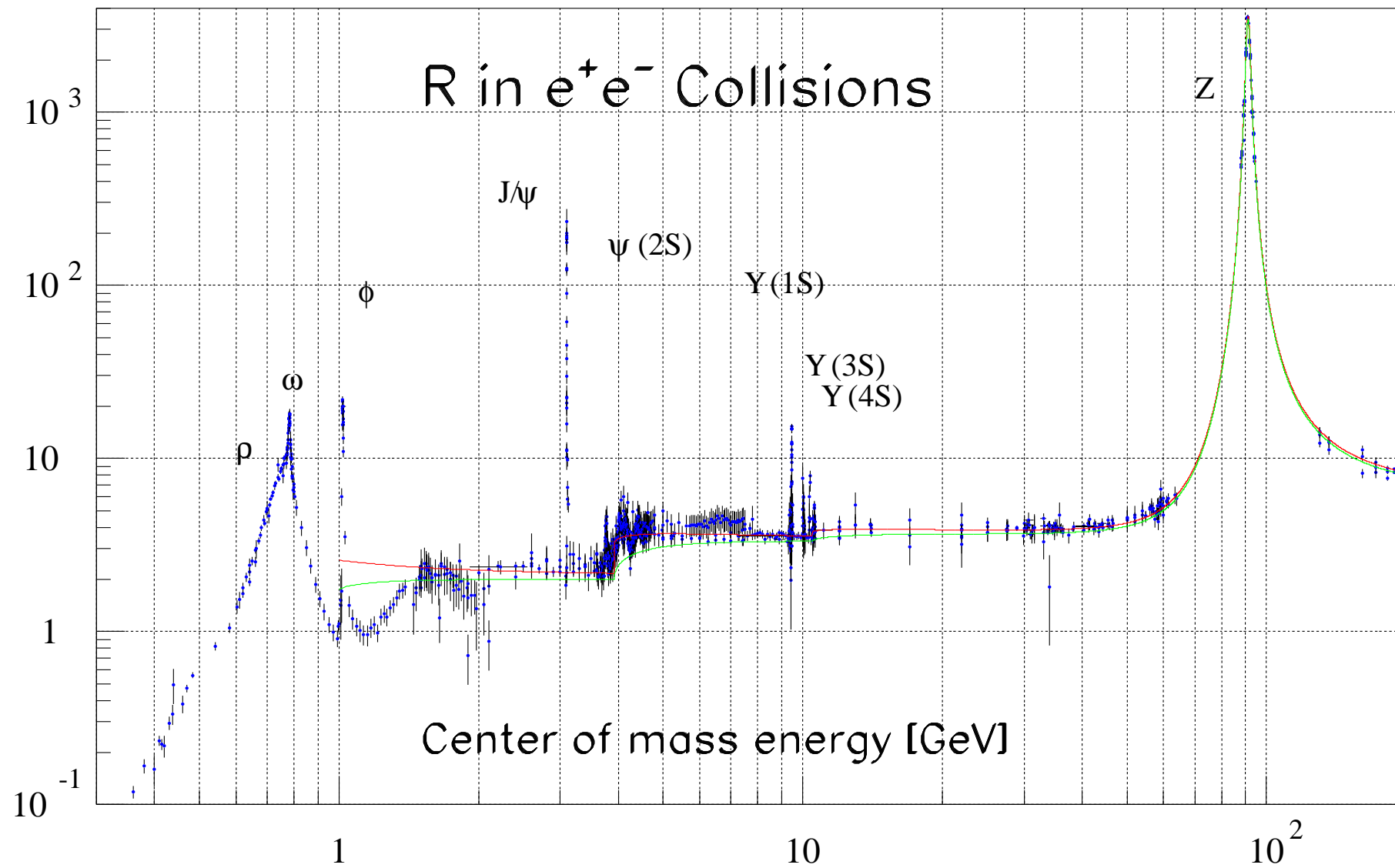


Fig. 6

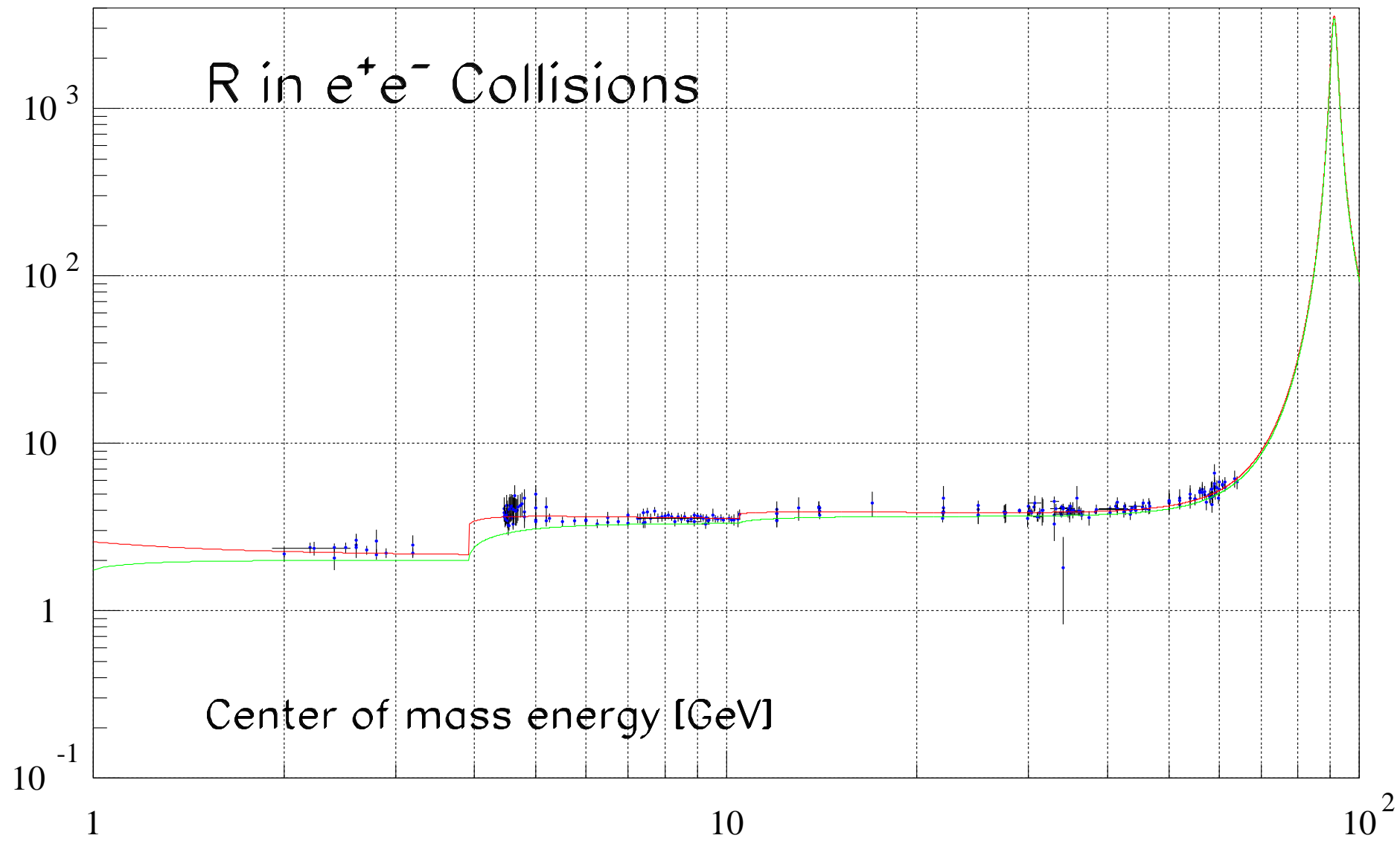


Fig. 7

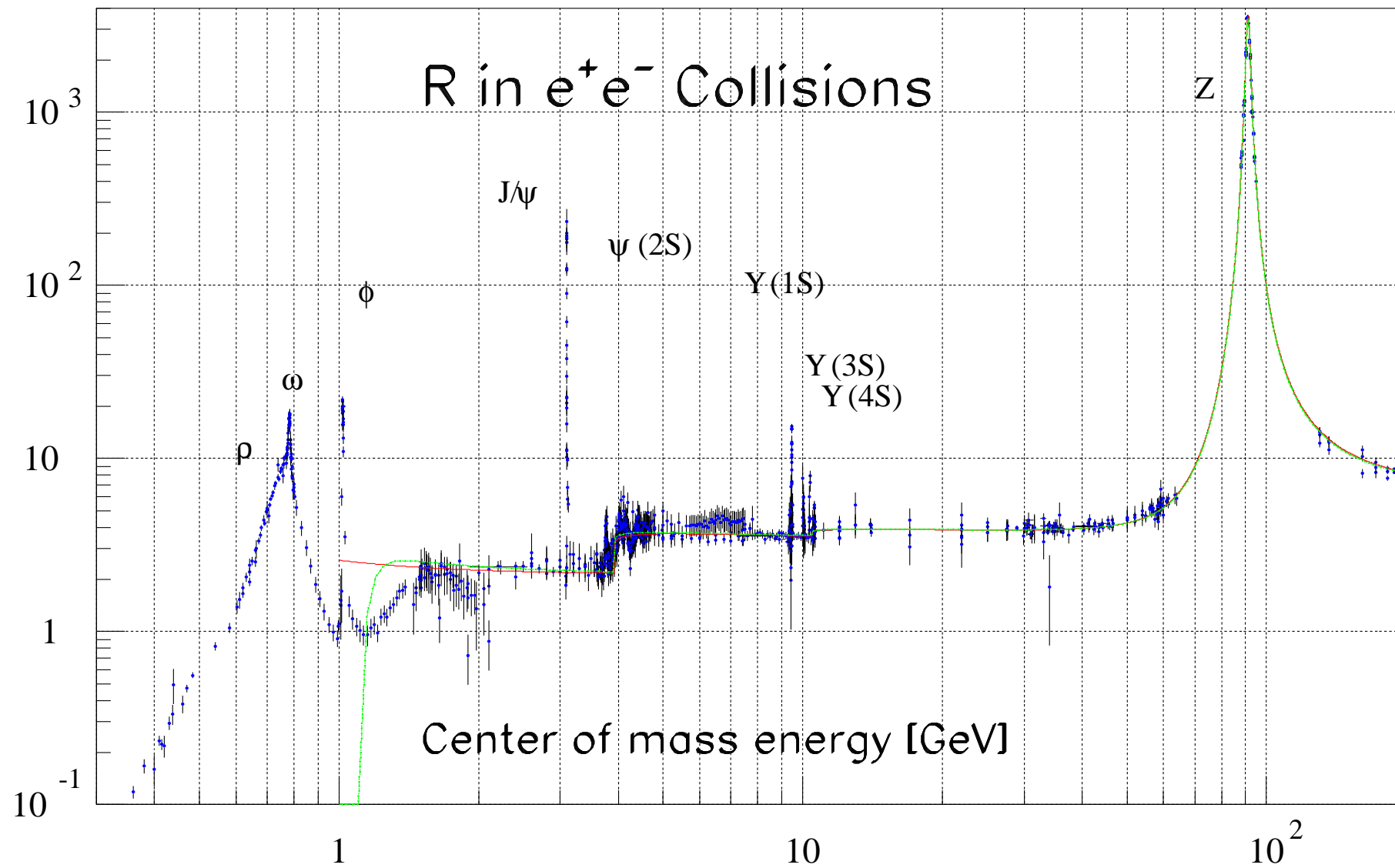


Fig. 8

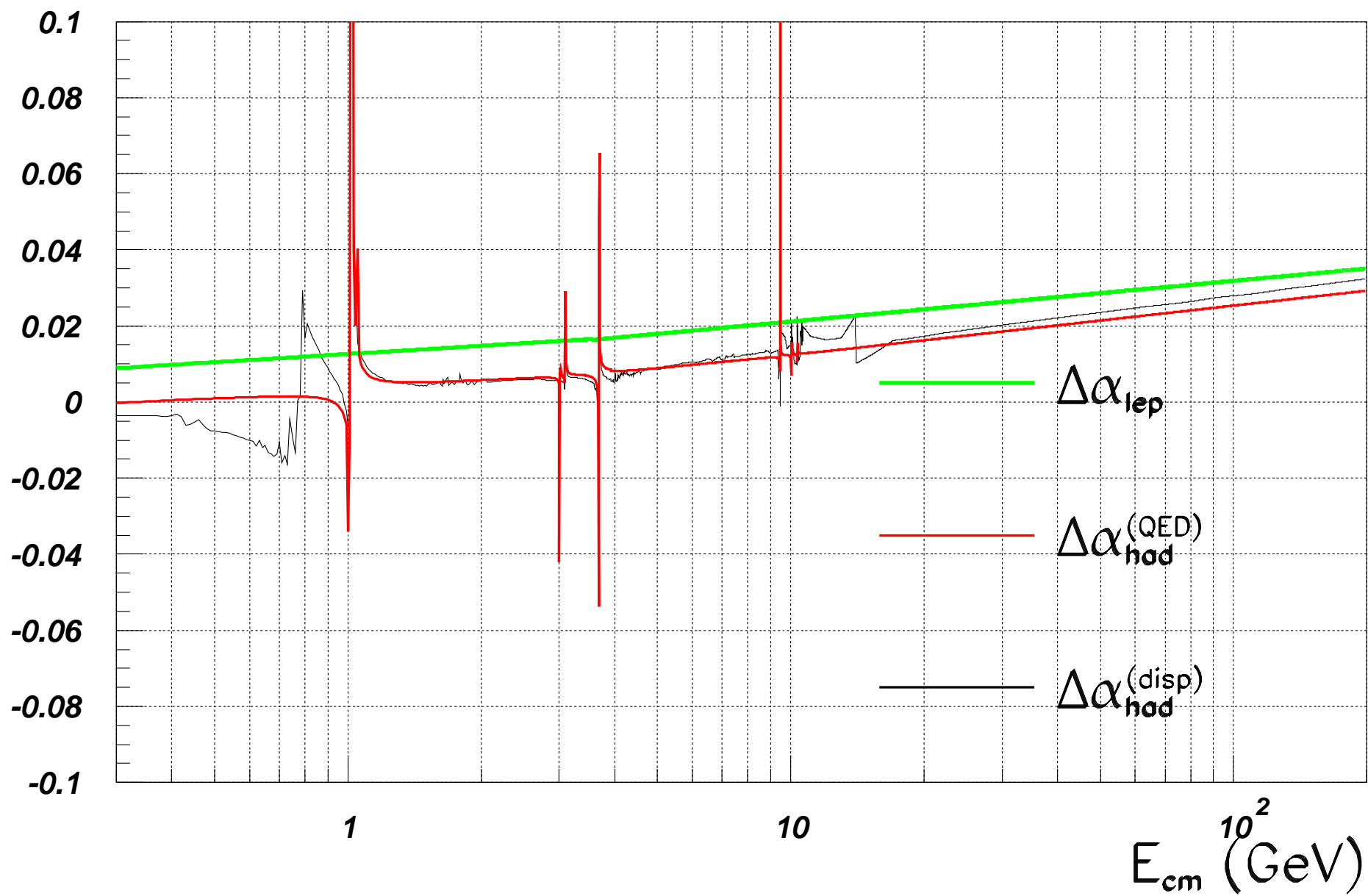


Fig. 9